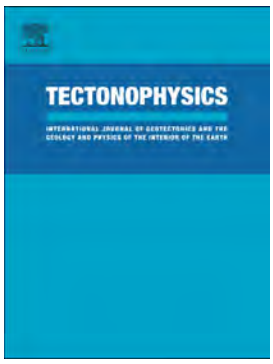

Earthquake damage orientation to infer seismic parameters in archaeological sites and historical earthquakes

Fidel Martín-González

PII: S0040-1951(18)30025-8
DOI: https://doi.org/10.1016/j.tecto.2018.01.013
Reference: TECTO 127751

To appear in: *Tectonophysics*

Received date: 3 November 2017
Revised date: 29 December 2017
Accepted date: 8 January 2018

Please cite this article as: Fidel Martín-González , Earthquake damage orientation to infer seismic parameters in archaeological sites and historical earthquakes. The address for the corresponding author was captured as affiliation for all authors. Please check if appropriate. Tecto(2017), https://doi.org/10.1016/j.tecto.2018.01.013

Earthquake damage orientation to infer seismic parameters in archaeological sites and historical earthquakes

Fidel Martín-González

Área de Geología. ESCET. Universidad Rey Juan Carlos. C/ Tulipán, s/n. Móstoles, 28933 Spain. *fidel.martin@urjc.es, +34914884583*

ABSTRACT

Studies to provide information concerning seismic parameters and seismic sources of historical and archeological seismic events are used to better evaluate the seismic hazard of a region. This is of especial interest when no surface rupture is recorded or the seismogenic fault cannot be identified. The orientation pattern of the earthquake damage (ED) (e.g., fallen columns, dropped key stones) that affected architectonic elements of cities after earthquakes has been traditionally used in historical and archaeoseismological studies to infer seismic parameters. However, in the literature depending on the authors, the parameters that can be obtained are contradictory (it has been proposed: the epicenter location, the orientation of the P-waves, the orientation of the compressional strain and the fault kinematics) and authors even question these relations with the earthquake damage. The earthquakes of Lorca in 2011, Christchurch in 2011 and Emilia Romagna in 2012 present an opportunity to measure systematically a large number and wide variety of earthquake damage in historical buildings (the same structures that are used in historical and archaeological studies). The damage pattern orientation has been compared with modern instrumental data, which is not possible in historical and archaeoseismological studies. From measurements and quantification of the orientation patterns in the studied earthquakes, it is observed that there is a systematic pattern of the earthquake damage orientation (EDO) in the proximity of the seismic source (fault trace) (<10km). The EDO in these earthquakes is normal to the fault trend (±15º). This orientation can be generated by a pulse of motion that in the near

fault region has a distinguishable acceleration normal to the fault due to the polarization of the S-waves. Therefore, the earthquake damage orientation could be used to estimate the seismogenic fault trend of historical earthquakes studies where no instrumental data are available.

Keywords Archaeoseismology, Palaeoseismology, Historical earthquakes, Earthquake damage, Quantification earthquake effects, Seismoscopes

1. Introduction

The base of the seismic hazard studies to mitigate future earthquake losses is to understand the earthquakes that hit a region in the past. Seismic catalogs incorporate information about past events by palaeoseismological, archaeological and historical studies. A multidisciplinary combination of historical, archaeological and palaeosismological data can provide insight into the seismogenic fault, recurrence, location and socioeconomic effects (e.g. Nur and Cline, 2000; Meghraoui et al., 2003; Michetti et al., 2005; Caputo and Helly, 2008; Karakhanian et al., 2008; Berberian et al., 2012; Udías, 2015). The study of the seismogenic fault by palaeoseismological studies of the surface rupture is one of the data sources (on-fault) that provide estimation of fault rupture, magnitude, location and recurrences for seismic catalogs. Unfortunately, catastrophic earthquakes of low to moderate magnitudes (M< 6.5) may not leave evidence of the surface ruptures (e.g., Pizzi and Scisciani, 2012; Martinez-Diaz, et al. 2012; Martin-Gonzalez et al, 2012; Mckey and Quigley, 2014). Therefore, for earthquakes for which seismogenic fault and surface ruptures have not been identified (because of the low to moderate magnitudes, blind faults, or just because it is not observed at the surface due to subsequent burial, erosion by surface processes or destruction by human activity), the evidence of the seismic events is found in the earthquake damage (ED) observed in historical or archaeological sites. Earthquake information can be obtained by the study off-fault of the ED recorded in historical and archaeological sites or in historical photographs and descriptions of the earthquakes (archaeoseismology, historical seismology) (e. g., Mallet, 1862; Musson, 1996; Korjenkov and

Mazor, 1999; Nur and Cline, 2000; Marco et al., 2003; Ambraseys, 2006; Galadini et al., 2006; Al-Tarazi and Korjenkov, 2007; Marco, 2008; Guidoboni and Ebel, 2009; Reicherter et al., 2009; Sintubin et al., 2010; Talwani, 2014; Stiros and Blackman, 2014; Kyriakides et al., 2016). This information, along with how the population felt the earthquake in many cases has been used to make estimations of the earthquake dates, locations of epicenters, focal depths, magnitude or intensity, ground shaking and seismic moments of the seismic events (Guidoboni and Ebel, 2009). All this information is crucial to evaluate the seismic hazard and regulatory seismic codes (Musson, 1996; Korjenkov and Mazor 1999, 2013; ASCE, 2010; Galadini et al., 2006).

In addition, as a consequence of the accident at the Fukushima Daiichi nuclear power plant (11th March 2011) and the lessons learned from that experience, the International Atomic Energy Agency (IAEA) undertook re-evaluation procedures for nuclear power plants and one of its strong recommendations is the use of ancient earthquakes data in seismic hazard assessments (IAEA, 2015).

Damage in architectonic elements of buildings (Fig. 1) are one of the effects observed after earthquakes, and they can remain in historical buildings and archaeological sites for years and even centuries as a witness of the earthquake. Such earthquake damage can be used to complete historical seismic catalogs and give information about earthquake parameters (e. g., Gasperini et al. 1999; Korjenkov and Mazor, 1999; Nur and Cline, 2000; Marco et al., 2003; Galadini et al., 2006; Marco, 2008; Reicherter et al., 2009; Sintubin et al., 2010; Rodriguez-Pascua et al., 2011; Hinzen et al., 2011). The orientation of the earthquake damage (e.g., fallen columns, toppled walls, conjugate fracture sets in walls, or dropped keystones in arches) in architectonic elements suffered due to an earthquake can be regarded as like structural seismoscope of the ground motion pulse (Mallet, 1862; Korjenkov and Mazor, 1999, 2013; Hinzen et al., 2016). For example, the generation of a dropped keystone (Fig. 1B, E and F) requires horizontal ground motion (Korjenkov and Mazor, 2003; Hinzen et al., 2016). In addition, from early studies like Mallet's reports in the 19th century, observations of the orientations of fractures in walls and of

tilted and collapsed walls were used to infer the epicenters and depths of the earthquakes (Mallet, 1862; Talwani, 2014). This information is especially important for earthquakes where non-instrumental information (e.g. seismometer information) is available (historical or archaeosismological earthquakes).

Commonly in historical and archaeoseismological studies the systematic orientation pattern of fallen columns and the tilting of architectural elements, at archaeological sites and historical buildings hit by earthquakes has been used to constrain seismic parameters like the epicenter location, the orientation of the P-waves, the orientation of the compressional strain and the kinematic of the fault (e.g. Mallet, 1862; Korjenkov and Mazor, 2009, 2013; Kazmer and Major, 2010, 2015). However, the parameters that are obtained from this orientation are contradictories between different authors. Thus, traditionally the earthquake damage orientation is interpreted as the orientation toward the epicenter and the P-waves (e.g. Mallet, 1862; Nur and Cline, 2000; Korjenkov and Mazor, 2009, 2013). Other authors propose that a systematic orientation of damage effects at a site indicates the direction of maximum-shortening and the orientation of seismo-tectonic strain ellipsoid (e.g., Giner-Robles et al., 2009; Korjenkov and Mazor, 1999; Rodriguez-Pascua et al., 2011). Others suggest that fallen columns oriented in the same direction indicate the kinematics of the fault (e.g., Nur and Burgess, 2008; Al-Tarazi and Korjenkov, 2007). Recently, others authors even question these relations (Hinzen 2009, 2011) because other factors like geometry, topography or irregularities in the columns could affect the fallen orientation and therefore is not clear the relation of falling directions to earthquake source location.

The catastrophic earthquakes of Lorca 2011, Emilia Romagna 2012 and Christchurch 2011 caused significant destruction of historical heritage (e.g., castles, churches, aqueducts, monumental monoliths, etc.) (Fig. 1). They also generated significant economic losses and fatalities, although the magnitudes of these earthquakes were moderate or low (never exceeded M 6.5, with no surface rupture) (i.e., IGME, 2011; Martinez-Diaz et al., 2012; Kaiser et al., 2012; ISPRA, 2012; Pizzi and Scisciani, 2012; Saraò, and Peruzza, 2012). These earthquakes

have allowed the systematic measurement a large number and wide variety of ED in historical buildings (the same structures used in historical and archaeological studies) and also a comparison of their orientations (Earthquake Orientation Damage-EDO) with modern instrumental data which is not possible in historical and archaeoseismological studies (seismogenic fault trend, focal mechanisms, accurate epicenter locations, magnitudes, etc.).

The aims of this work are: (1) Check if an orientation pattern of the earthquake damage (EDO) is recorded in historical building after an earthquake and if it can be systematically measured and quantified. (2) Take advantage of the instrumental data of the modern earthquakes, analyzing if the orientation correlates with the seismic parameters that are proposed in the literature for historical and ancient earthquakes. (3) Evaluate if the seismogenic fault can be constrain by analyzing the EDO in archaeological or historical sites in the cases where no surface rupture is identified or non-instrumental data are available.

2. Methods

The three regions aforementioned hit by earthquakes were selected (Table 1) due to the available instrumental data and to the presence of historic buildings with unreinforced masonry structures (the same structures used in historical and archaeological studies) (Fig. 1).

Oriented damage due to earthquakes has been described at archaeological sites and in historical cities affected by earthquakes (e.g. Stiros, 1996; Korjenkov and Mazor, 1999; Ambraseys, 2006; Galadini et al., 2006; Marco, 2008; Rodriguez-Pascua et al., 2011; and references therein) (Fig. 1). In this study, six different types of ED have been recognized based on the extensive literature about damage that can offer orientation information of the ground motion. A total of 423 measurements of oriented earthquake damage at 19 sites were obtained in the seven field campaigns conducted during this study (Table 2). Following the literature the six ED recognized are described:

(a) Fallen and tilted walls (Fig. 1C): Systematic directional tilting and toppled walls are the most conspicuous consequences of the horizontal movement of the ground shake. In these cases the lower part of the structure moved with the ground in the direction of the particular ground movement, whereas the upper part did not move due to inertia. Therefore, the preservation of the walls after falling in a preferred direction indicates the direction of the ground motion and this direction has been used, for example, to locate historical epicenters (e.g., Korjenkov and Mazor, 1999, 2003, 2013; Rodriguez Pascua et al., 2011).

(b) Conjugated fractures and horizontal fractures in walls (Fig. 1B). Penetrative fractures with conjugate orientation (fractures in an X configuration affecting masonry and brick walls are common phenomena among earthquake damage patterns (e.g. Stiros 1996; Al-Tarazi and Korjenkov, 2007; Korjenkov and Mazor 2013, 1999). The response of a wall to an earthquake depends on the orientation relative to the ground motion direction (Stiros, 1996), thus ground motion perpendicular to the wall will generate horizontal fractures and finally topple it, but ground motion acting parallel to a wall generate conjugated fractures in X configuration (e.g., Stiros, 1996; Rodriguez Pascua et al., 2011).

(c) Dipping broken corners or chipping marks (Fig. 1H). Dipping broken corner or chipping marks (e.g., Stiros, 1996 and Marco, 2008) are broken triangular shapes that occur in the masonry blocks corners by the earthquake shaking. Rodriguez-Pascua et al. (2011) indicate that the dip direction of the broken corner is parallel to the ground motion peak.

(d) Dropped keystones in arches, windows, doors, bridges and arcs (Fig. 1 B, E, F). Downward moved keystones of arches, large windows, bridges and doors are common in regions hit by earthquakes (e.g., Korjenkov and Mazor, 2003, 2013, Marco, 2008). Hinzen et al. (2016) indicate that arches are architectonic elements essential to archaeoseismological studies because dropped keystones are clear indications of a seismogenic cause and a horizontal ground motion can only cause it. Hinzen et al, (2016) do not relate the dropped keystone to any specific ground motion direction but others (e.g., Rodríguez-Pascua et al., 2011) stablish a relation of less than 45º between the arch orientation and the ground motion direction.

(e) Fallen columns (Fig. 1 A and D). Fallen and oriented columns or the columns fallen drums (when imbricated) are common features associated with earthquakes (e.g. Stiros, 1996; Korjenkov and Mazor, 2013), especially if groups of monolithic columns fell aligned, all in the same direction. This orientation of fallen columns have been used widely in the literature to calculate epicenter location or fault kinematics (e.g. Nur and Burgess, 2008; Kazmer and Mayor, 2015; Korjenkov and Mazor, 2009, 2013). Others authors call into question these relations because other factors like geometry, topography or irregularities in the columns can affect the fallen orientation and therefore is not clear relation of falling directions to earthquake source location (Hinzen 2009, 2011).

(f) Displaced masonry blocks and tombstones (Fig. 1 G and D). If the action of roots and soil flow can be excluded, then only earthquakes can generate forces large enough to displace large heavy blocks by horizontal sliding (e.g., Marco, 2008; Rajendran et al., 2013).

In this paper, all orientation of damage has been measured *in situ* with a compass. In other studies (Guidoboni and Ebel, 2009), the orientation of the ED can be also obtained from other scientific sources utilized in the study of historical earthquakes, like scientific reports, historical documents describing the earthquake, archaeological drawings, historical earthquake cartography, historical photographs, films from archives and even unwritten sources.

The frequency of the observations of damage orientation in a given direction is represented in rose diagrams (Fig. 2, 3 and 4) (Table 2). A range of uncertainty in every ED has been considered according to the degree of freedom in which the structural element can be oriented by the ground motion pulse. According to the shape of an architectonic element, it may have only certain degrees of freedom to fall in an oriented manner related to a range of ground motion (Fig. 5). For example, elements with quadrangular or rectangular bases (e.g., obelisks, pinnacles, etc.) have 90º of uncertainty to record the orientation of an incoming pulse. Others elements such as walls or headstones have only two possible direction of falling with an uncertainty of 180º in the orientation of the ground motion pulse that caused the fall (Fig. 5A). In the same way, a keystone can drop only if the arch that contains it is oriented parallel to the

pulse orientation but it does not slide if the ground movement is normal to the arch. For this reason, the ED have been sorted into four groups according to the ranges of uncertainty in which they can be oriented by the ground acceleration pulse: (a) two degrees of freedom (tilted and toppled walls, horizontal and conjugates fractures in walls) (180º), (b) four degrees of freedom (dipping broken corners, dropped keystones, fallen columns and obelisks with square bases) (90º), (c) six degrees of freedom (fallen columns and monoliths with hexagonal bases) (60º), (d) all degrees of freedom (displaced masonry blocks, fallen columns with round bases)(20º). The azimuths have been represented in rose diagrams that show the entire possible range for the incoming pulse orientation (Fig. 2, 3 and 4).

The second aim of this work is to compare the EDO observed in the three earthquakes with the earthquake parameters that are proposed in the literature for historical and ancient earthquakes (orientation toward the epicenter, P-waves, fault displacement and orientation of the maximum compressional strain). In this work, epicenter location and seismic parameters were obtained from the USGS and from the published literature referenced (Fig. 2, 3 and 4) (Table 1) (Beavan et al., 2012; Martinez-Diaz et al., 2012; Saraò and Peruzza, 2012). The strike, dip, and rake angle of the fault has been obtained from the focal mechanisms published by the USGS. The P-waves have been modeled by the spatial distribution of the radiation of seismic waves for a double-couple earthquake point source (P-waves for each event) using the online code of Scherbaum et al. (2015).

3. Results

The results are summarized in table 2 and figures 2, 3 and 4:

3.1. Lorca Earthquake 2011 (M5.1 Spain)

On May 11th, 2011, a M 5.1 earthquake hit the city of Lorca in south-eastern Spain (Fig. 2 and Table 2). It had an intensity of VIII (USGS)(Table 1). Focal mechanism solutions indicate a

strike-slip fault with a reverse component of slip with ENE-WSW-trending (N54º) (USGS). This trend is sub-parallel to the Alhama de Murcia Fault (AMF), which is the proposed seismogenic fault (IGME, 2011, Martinez-Diaz et al., 2012; Vissers and Meijninger, 2011). Reports soon after the earthquake reported no surface rupture in the region (IGME, 2011).

The damage orientation trends are NNW-SSE (N335º- N150º) (Table 2). Around the fault and for all sites the orientation of the damage remains systematically normal to the seismogenic fault (Fig. 2).

3.2. Emilia Romagna Earthquakes 2012 (M6-M5.8 Italy)

On May 2012 two earthquakes hit the Emilia-Romagna Region of northern Italy (Fig. 3). On May 20th a M 6 and on 29th a second strong event of M 5.8 hit the same region. Both had a maximum intensity of VIII (USGS) (Table 1). Both focal mechanism solutions indicate low-angle reverse faulting with WNW-ESE-trending (N100º) fault plane (USGS)(Table 1). These events occurred along the E-W-striking outermost active sector of the northern Apennines thrust front buried by a thick Miocene-Quaternary foreland basin (Pizzi and Scisciani, 2012; Carminati and Doglioni, 2012). Reports soon after the earthquakes reported the absence of surface rupture (ISPRA, 2012; Pizzi and Scisciani, 2012).

The EDO trends NNE-SSW (N225º-N45º) (Table 2), except for two sites (Cavezzo, and San Felice sul Panaro) which do not have a preferred orientation. Around the faults, the EDO is normal to the seismogenic faults (N 10º-30º, NNE-SSW). The EDO is less systematic in sites located south of the epicenters (San Felice Sul Panaro and Crevalcore) and sites located more than 10km away from the fault (Crevalcore site) (Fig. 3).

3.3. Christchurch Earthquakes 2011 (M6.0-M5.9-M5.9, South Island of New Zealand)

Between February and December 2011, Christchurch, the second largest city of New Zealand, was hit by a sequence of earthquakes (22 February 2011 (M 6.1; IX), 13 June 2011 (M 5.9; VIII and 23 December 2011 (M 5.9; VII) (USGS)(Fig. 4). The 2011 main earthquake took place on previously undetected blind faults beneath Christchurch and no surface rupture was reported (Kaiser et al., 2012; Beavan et al., 2012). Focal mechanism solutions for the Christchurch February and December earthquakes are quite similar, a reverse with strike-slip component fault trending ENE-WSW, dipping to the southeast. The event of 13th June (M 6.0) was a NNW-SSE, left-lateral strike slip fault (Table 1).

Two general damage orientations are observed: NNW-SSE and WSW-ENE (N170º-N75º) (Table 2). NNW-SSE orientation is manifested more clearly around the fault of the main event (22-02-2012) and perpendicular to the seismogenic fault (ENE-WSW), while at sites located eastward, the WSW-ENE orientation is more predominantly recorded (Fig. 4). These variations in the directions would indicate the influence of each of the faults on the nearest sites. As a result of the multiples sequences the orientation results are obliterated.

4. Discussion

In the three regions affected by earthquakes studied in this work (Lorca 2011, Christchurch 2011 and Emilia Romagna 2012), the orientations of the damage caused by the earthquakes in historical architectonic elements were measured. It is observed that damage is systematically orientated in the proximity of the fault (less than 10 km) (Table 2) (Fig. 2, 3 and 4).

The earthquake damage orientations (EDO) were compared to the proposed orientations of earthquake parameters published in the literature: The epicenter location, The P-waves radiation (if it was the cause, the EDO should follow the radiation patterns, which have been modelled for every event with software from Scherbaum et al., 2015); The fault displacement (if it was the

cause, the EDO should be oriented following the the seismogenic fault kinematic-slip vector); The orientation of the maximum compressional strain (if it was the cause, the EDO should be oriented following maximum compressional strain). Finally, the damage orientation has been compared with the fault trend. Therefore, in Figure 6 the EDO is plotted versus the orientation (direction 0º-180º) of the (a) seismogenic fault trend (normal), (b) orientation towards the epicenter (P-waves), (c) fault displacement and (d) orientation of the maximum compressional strain. In the chart, the line represents the same orientation for the values of the two axes.

Comparing the data, it can be observed (Fig. 6, Table 2): (1) The EDO is not oriented toward the epicenters (as it can be observed in the dispersion of the circles in Fig. 6). (2) The EDO is not parallel to the P-Waves (Fig. 2, 3 and 4). (3) The EDO does not present the same orientation that the maximum shortening or compressional strain (as it can be observed in the dispersion of the triangles in Fig. 6). (4) The EDO does not present orientations that follow the kinematic or movement of the fault (as it can be observed in the dispersion of the square points in Fig. 6). Finally, the EDO is normal to the seismogenic fault trend (pentagons in Fig. 6).

Ground motion is one of the main factors responsible for earthquake damage (Somerville et al., 1997). Somerville et al., (1997) established that the propagation of fault rupture toward a site causes most of the seismic energy from the rupture to arrive in a ground motion pulse. This pulse of motion represents the cumulative effect of almost all of the seismic radiation from the fault. The radiation pattern is oriented in the direction normal to the fault and it is dominated by the fault characteristics (Somerville et al., 1997). These studies also report that in the near fault region, earthquake ground motion has distinguishable acceleration pulse normal to the fault due to the polarization of the S-waves (Somerville et al., 1997; Somerville, 2003). This ground motion pulse is enhanced when directivity in rupture takes place, which was the case in the three studied cases (Kaiser et al., 2012; Lopez Comino et al., 2012 Saraò and Peruzza, 2012). For this reason, this pulse could be responsible for the EDO in the three cases studied. It records the horizontal main ground motion, an important factor for design verification of historical structures and an important factor in the design of critical facilities and regulatory seismic codes

(e.g., California Building Code, section 1615A.1.25; ASCE, 2010). Therefore, surveying and analyzing the EDO generated in an historical earthquake or at archaeological sites, it could be used as a quick and preliminary way to infer the seismogenic fault trend and constrain the seismogenic fault from other active candidate faults of the region with different trends, because the seismogenic fault should be normal to the EDO. This is of special interest in regions where there is not seismic fault rupture identifiable for the earthquake. When the EDO is not clearly observed it could indicate that the near-fault effects are attenuated, this is observed in the effects located more than 10 km far in Emilia Romagna earthquakes (Fig. 3). Therefore, if no orientation damage is observed, it could also offers information: indicating that the site can be more than 10 km from the epicenter, neutral directivity or multiple events that obliterated the orientations as it was observed in Christchurch earthquakes.

5. Conclusions

Information of the seismogenic source of ancient earthquakes can be obtained by quantifying earthquake damage orientation (EDO) in archaeological sites, historical buildings or historical photographs. This information is of value especially in regions were no fault surface rupture can be identified. This damage can act like structural seismoscopes recording the ground motion pulse, important factor in the design of critical facilities and regulatory seismic codes. However, in the literature, the parameters that can be obtained from the earthquake damages are contradictory depending on the authors and even call into question any relation with the earthquake damage. In the three regions affected by earthquakes studied in this work (Lorca 2011, Christchurch 2011 and Emilia Romagna 2012), the damage caused by the earthquake in historical buildings is systematically oriented in the proximity of the fault (less than 10 km). The EDO is normal (±15º) to the fault trend. The three studied cases show that: (1) The EDO is not oriented toward the epicenters. (2) The EDO is not parallel to the P-waves. (3) The EDO do not present the same orientation as that of the maximum shortening or compressional strain. (4)

The EDO is not oriented according to the kinematic of the fault. Therefore, if the EDO is systematically oriented, it can be interpreted as the result of the ground motion, which has an acceleration pulse normal to the fault. This pulse in near fault sites is mainly dominated by the source characteristics with a distinguishable acceleration pulse normal to the fault due to the polarization of the S-waves, therefore can be used to infer the seismic parameters of the source. This way, when the earthquake damage orientation is observed in an archaeological site, it could be used as a quick and preliminary way to estimate the seismogenic fault trend from the other candidate faults with different trends. This information combined with historical and archaeological studies that can determine the timing, intensity and location of the earthquake are of great value in seismic hazard studies where no instrumental data are available and the fault rupture is not recognized.

Acknowledgments

This work was partially supported by the Spanish Government (MINECO-FEDER) projects CGL2011-14925-E and CGL2015-70970-P. The author expresses his appreciations to M.A Rodriguez-Pascua, R. Pérez-Lopez, A. Marquez and F. Barrio and for critically reading the manuscript and making several useful remarks. The author also expresses his appreciations to the reviewers (Dr. Rajendran and Dr. Korjenkov) and editors for their constructive comments to improve the manuscript. Thanks are given to the firefighter teams and authorities during the fieldwork.

References

Al-Tarazi, E.A., Korjenkov, A.M., 2007. Archaeoseismological investigation of the ancient Ayla site in the city of Aqaba, Jordan. Nat Hazards. 42, 47–66, doi, 10.1007/s11069-006-9045-6

Ambraseys, E., 2006. Earthquakes and archaeology. J Archaeol Sci. 33, 1008-1016.

ASCE, 2010. American Society of Civil Engineer. Minimum Design Loads for Buildings and Other Structures, ASCE/SEI 7-10. American Society of Civil Engineers, Reston, VA, 650 pp.

Beavan, J., Motagh, M., Fielding, E.J., Donnelly, N., Collett, D., 2012. Fault slip models of the 2010–2011 Canterbury, New Zealand, earthquakes from geodetic data and observations of postseismic ground deformation. New Zeal J Geolo Geop. 55, 207–221, doi, 10.1080 /00288306.2012.697472.

Berberian, M., Shahmirzadi, S.M., Nokandeh J., Djamali M., 2012. Archaeoseismicity and environmental crises at the Sialk Mounds, Central Iranian Plateau, since the Early Neolithic. J Archaeol Sci. 39, 2845-2858

Caputo R., Helly B., 2008. The use of distinct disciplines to investigate past earthquakes Tectonophysics. 453, 7–19

Galadini F., Hinzen K. G., Stiros S., 2006. Archaeoseismology, Methodological issues and procedure. Journal of Seismology. 10, 395–414, DOI 10.1007/s10950-006-9027-x

Gasperini, P., Bernadini, F., Valensise, G., Boschi, E., 1999. Defining seismogenic sources from historical earthquake felt reports. B Seismol Soc Am. 89, 94-110.

Giner-Robles, J.L., Rodríguez-Pascua, M.A., Pérez-López, R., Silva, P.G., Bardají, T., Grützner, C., Reicherter, K., 2009. Structural Analysis of Earthquake Archaeological Effects (EAE), Baelo Claudia Examples (Cádiz, South of Spain), In, I International Workshop on Earthquake Archaeology and Palaeoseismology. Instituto Geológico y Minero.

Guidoboni, E., Ebel, J.E., 2009. Earthquakes and Tsunamis in the Past, A Guide to Techniques in Historical Seismology. Cambridge University Press. 590pp.

Hinzen K., Fleischer, C., Reamer, K., Schreiber, S., Schütte, S., Yerli, B., 2011. Quantitative methods in archaeoseismology. Quaternary International, 242, 31-41

Hinzen, K. G., 2011. Sensitivity of earthquake-toppled columns to small changes in ground motion and geometry: Isr. J. of Earth Sci. 58, 309-326.

Hinzen, K.G., 2009. Simulation of toppling columns in archaeoseismology: Bulletin of the Seismological Society of America. 99, 2855-2875.

Hinzen, K.G., Schwellenbach I., Schweppe, G., Marco, S., 2016. Quantifying Earthquake Effects on Ancient Arches, Example, The Kalat Nimrod Fortress, Dead Sea Fault Zone. Seismol. Res. Lett. 87, no. 3,751-764. doi, 101785/0220150282

IAEA, 2015. The contribution of palaeoseismology to seismic hazard assessment in site evaluation for nuclear installations. International Atomic Energy Agency IAEA-TECDOC series, 1767.

IGME, 2011. Martinez-Diaz, J.J., Rodriguez-Pascua, M.A., Perez Lopez, R., Garcia Mayordomo, J., Giner Robles, J.L., Martin-Gonzalez, F., Rodriguez Peces, M., Alvarez Gomez, J.A. and Insua Arevalo, J.M. 2011. Informe Geológico Preliminar del Terremoto de Lorca del 11 de mayo del año 2011, 5.1 Mw, Instituto Geológico y Minero de España.

ISPRA, 2012. Geological Effects Induced by the Seismic Sequence Started on May 20, 2012, in Emilia (Mw 5.9). Preliminary Report, Open file report. Servizo Geologico d'Italia.

Kaiser, A., Holden, C., Beavan, J., Beetham, D., Benites, R., Celentano, A., Collett, D., Cousins, J., Cubrinovski M., Dellow G., Denys P., Fielding E., Fry B., Gerstenberger, M., Langridge, R., Massey, C., Motagh, M., Pondard, N., McVerry, G., Ristau, J.,

Stirling, M., Thomas, J., Uma, S.R., Zhao, J., 2012. The Mw 6.2 Christchurch earthquake of February 2011, preliminary report. New Zeal J Geolo Geop. 55, 67-90

Karakhanian, A.S., Trifonov, V.G., Ivanova, T.P., Avagyan, A., Rukieh, M., Minini, H., Dodonov A.E., Bachmanov, D.M., 2008. Seismic deformation in the St. Simeon Monasteries (Qalat Siman), Northwestern Syria. Tectonophysics. 453, 122–147

Kázmér M., Major B., 2010. Distinguishing damages from two earthquakes—Archaeoseismology of a Crusader castle (Al-Marqab citadel, Syria).The Geological Society of America Special Paper. 471, 185-198.

Kazmér, M., Major, B., 2015. Safita castle and rockfalls in the 'dead villages' of coastal Syria – an archaeoseismological study. Comptes Rendus Geoscience. 347, 181–190.

Korjenkov A. M., Mazor E., 2013. The Features of the Earthquake Damage Patterns of Ancient City Ruins in the Negev Desert, Israel. Geotectonics. 47, 52–65, doi, 10.1134/S0016852113010032

Korjenkov, A.M., Mazor E., 1999. Seismogenic origin of ancient Avdat ruins, Negev Desert, Israel. Nat Hazards. 18,193–226

Korjenkov, A.M., Mazor, E., 2003. Archaeoseismology in Mamshit (Southern Israel): Cracking a Millennia-old Code of earthquakes Preserved in Ancient Ruins. Archäologischer Anzeiger. 2, 51-82

Kyriakides N., Lysandrou V., Agapiou A., Illampas, R., Charalambou,s E., 2016. Correlating damage condition with historical seismic activity in underground sepulchral monuments of Cyprus, J Archaeol Sci., Reports. http,//dx.doi.org/10.1016/j.jasrep.2016.07.007

Lopez-Comino, J.A., Mancilla, F., Morales, J., Stich, D., 2012. Rupture directivity of the 2011, Mw 5.2 Lorca earthquake (Spain). Geophysical Research Letters. 39, L03301, doi,10.1029/2011GL050498.

Mackey, B.H., Quigley, M.C., 2014. Strong proximal earthquakes revealed by cosmogenic 3He dating of prehistoric rockfalls, Christchurch, New Zealand. Geology. 42, 975-978, doi, 10.1130/G36149.1

Mallet, R., 1862. Great Neapolitanian Earthquake of 1857. The First Principles of Observational Seismology. Chapman and Hall, London. 831 pp.

Marco S., 2008. Recognition of earthquake-related damage in archaeological sites, Examples from the Dead Sea fault zone. Tectonophysics. 453, 148–156.

Marco, S. Hartal, M., Hazan N., Lev, L., Stein, M., 2003. Archaeology, history, and geology of the A.D. 749 earthquake, Dead Sea transform. Geology. 31, 665-668, doi, 10.1130/G19516.1

Martinez-Diaz, J.J., Bejar-Pizarro, M., Alvarez-Gomez J., Mancilla, F., Stich, D., Herrera, G., Morales, J., 2012. Tectonic and seismic implications of an intersegment rupture. The damaging May 11th 2011 Mw 5.2 Lorca, Spain, earthquake. Tectonophysics. 547, 28–37, doi, 10.1016/j. tecto.2012.04.010.

Martín-González, F., Antón, L., Insua, J.M., De Vicente, G., Martínez- Díaz, J.J., Muñoz-Martín, A., Heredia, N., Olaiz, A., 2012. Seismicity and potentially active faults in the Northwest and Central-West Iberian Peninsula. Journal of Iberian Geology. 38, 53–69, doi: 10.5209/ rev_JIGE.2012.v38.n1.39205.

Meghraoui, M., Gomez, F., Sbeinati R., Van der Woerd, J., Mouty, M., Darkal, A. N., Radwan, Y., Layyous, I., Al Najjar, H., Darawcheh, R., Hijazi, F., Al-Ghazzi, R., Barazangi, M., 2003. Evidence for 830 years of seismic quiescence from palaeoseismology, archaeoseismology, and historical seismicity along the Dead Sea fault in Syria. Earth Planet. Sci. Lett. 210, 35–52.

Michetti, A.M. Audemard F. A., Marco S., 2005. Future trends in palaeoseismology, Integrated study of the seismic landscape as a vital tool in seismic hazard analyses. Tectonophysics. 408, 3-21 doi,10.1016/j.tecto.2005.05.035

Musson, R., 1996. Determination of parameters for historical British earthquakes. Annali di Geofisica. 34, 1041-1047

Nur, A., Burgess, D., 2008. Earthquakes, archaeology and the wrath of God. Princeton University Press, Princeton. 328pp.

Nur, A., Cline, E., 2000. Poseidon's Horses, Plate Tectonics and Earthquake Storms in the Late Bronze Age Aegean and Eastern Mediterranean. J Archaeol Sci. 27, 43–63

Pizzi A., Scisciani V., 2012. The May 2012 Emilia (Italy) earthquakes, preliminary interpretations on the seismogenic source and the origin of the coseismic ground effects. Annals of Geophysics. 55, no. 4, 751-757, doi, 10.4401/ag-6171

Rajendran, C. P., Rajendran, K., Sanwal, J., Sandiford, M., 2013. Archaeological and Historical Database on the Medieval Earthquakes of the Central Himalaya, Ambiguities and Inferences Seismol. Res. Lett. 84, no. 6, 1098-1108, doi, 10.1785/0220130077

Reicherter, K., Michetti, A.M., Silva, P. (eds.), 2009. Palaeoseismology, Historical and praehistorical records of earthquake ground effects for seismisc hazard assessment. Geological Society of London, Special Publications, 316

Rodriguez-Pascua, M.A., Perez-Lopez, R., Silva, P.G., Giner- Robles, J.L., Garduno-Monroy, V.H., Reicherter, K., 2011. A Comprehensive Classification of Earthquake Archaeological Effects (EAE) for Archaeoseismology. Quaternary Internationa. 242, 20-30.

Saraò, A., Peruzza, L., 2012. Fault-plane solutions from moment-tensor inversion and preliminary Coulomb stress analysis for the Emilia Plain. Annals of Geophysics. 55, 4, 2012; doi, 10.4401/ag-6134.

Scherbaum, F., Kuehn, N., Zimmermann, B., 2014. Radiation Pattern for Double-Couple Earthquake Sources, the Wolfram Demonstrations Project, http,//demonstrations.wolfram.com/RadiationPatternForDoubleCoupleEarthquakeSources/ (April 2016)

Sintubin, M., Stewart, I.S., Niemi, T.M., Altunel, E., 2010. Ancient Earthquakes, Geological Society of London, Special Paper. 471, 279 pp.

Somerville, P.G., 2003. Magnitude scaling of the near fault rupture directivity pulse, Physics of the Earth and Planetary Interiors. 137, 201–212, doi,10.1016/S0031-9201(03)00015-3

Somerville, P.G., Smith, N.F., Graves, R.W., Abrahamson, N.A., 1997. Modification of empirical strong ground motion attenuation relations to include the amplitude and duration effects of rupture directivity. Seismol Res Lett. 68, no.1, 199–222.

Stiros S. C., Blackman D. J., 2014. Seismic coastal uplift and subsidence in Rhodes Island, Aegean Arc, Evidence from an uplifted ancient harbour Tectonophysics. 611, 114–120 doi,10.1016/j.tecto.2013.11.020

Stiros, S., 1996. Identification of earthquakes from archaeological data, Methodology, criteria and limitations, in, Archaeoseismology, (S. Stiros and R. Jones Editors),Fitch Laboratory Occasional Paper 7, 129–152, Oxford.

Talwani P., 2014. The Impact of the Early Studies Following the 1886 Charleston Earthquake on the Nascent Science of Seismology Seismol. Res. Lett. 85, no. 6, 1366-1372, doi, 10.1785/0220140094

Udías A., 2015. Historical Earthquakes (before 1755) of the Iberian Peninsula in Early Catalogs Seismol. Res. Lett. 86, 999-1005, doi, 10.1785/0220140200

Vissers, R.L.M., Meijninger, B.M.L., 2011. The 11 May 2011 earthquake at Lorca (SE Spain) viewed in a structural-tectonic context. Solid Earth. 2, 199-204

Figure Captions

Fig. 1. Examples of oriented earthquake damage. A, Fallen Columns (Mirandola cemetery, Italy, 2012); B, Conjugated fracture sets and dropped keystones in windows (Castello San Felice Sul Panaro, Italy, 2012); C, Fallen wall (Finale Emilia, Italy, 2012)(notice how the perpendicular wall remains intact). D, Fallen columns (obelisks, funeral monoliths, crosses). (Bromley cemetery of Christchurch, New Zealand, 2011); E, Dropped Keystone (Santiago Church of Lorca, Spain, 2011); F, Dropped keystone in Window (Paso Azul Church of Lorca, Spain, 2011); G, Displaced masonry blocks (Torre del Espolón in Lorca castle, Spain, 2011); H, Dipping broken corners (Gate in the Historic cemetery of Lorca, Spain, 2011)

Fig. 2. Lorca Earthquake, Spain (2011). The structural framework and seismicity data (star represents the epicenter of the main shock; focal mechanism; date and magnitude) (USGS). P radiation patterns model with software from Scherbaum *et al.,* 2015. Arrows in the wave radiation model indicate the directivity. Rose diagrams represent the damage orientation, petals of 10º (Nº number of ED measured). The rectangle represents the fault rupture plane inferred by RADAR interferometry (Martinez-Diaz *et al.,* 2012)

Fig. 3. Emilia Romagna Earthquakes, Italy (2012). The structural framework and seismicity data (star represents the epicenter of the main shock; focal mechanism; date and magnitude) (USGS). P radiation patterns model with software from Scherbaum *et al.,* 2015. Arrows in the wave radiation model indicate the directivity. Rose diagrams represent the damage orientation, petals of 10º (Nº number of ED measured). The rectangle represents the fault rupture plane inferred by moment-tensor inversion and Coulomb stress analysis (Saraò and Peruzza, 2012)

Fig. 4. Christchurch Earthquakes, New Zealand (2011). It is showed the structural framework and seismicity data (star represents the epicenter of the main shock; focal mechanism; date and magnitude) (USGS). P radiation patterns model with software from Scherbaum *et al.,* 2015. Arrows in the wave radiation model indicate the directivity. Rose diagrams represent the damage orientation, petals of 10º (Nº number of ED measured). The rectangle represents the fault rupture plane inferred by geodetic data for the main shocks (Beavan *et al.,* 2012).

Fig. 5. A.-Example of three architectonic elements with oriented damage (dropped keystones, fallen obelisks with square bases and toppled walls), showing the range of uncertainty in which they can be oriented by the ground motion pulse (arrows). According to the shape of the architectonic elements, they may have different degrees of freedom to fall oriented or record the pulse. B.-The overlapping of the uncertainty ranges indicates the direction of incoming pulse common for all the elements. C.-The azimuths have been represented in a frequency plots rose diagrams, considering the whole range equally valid for the incoming pulse orientation.

Fig. 6. Earthquake damage orientation (EDO) (0º-180º) plotted versus the orientation of, (a) seismogenic fault trend (normal), (b) orientation towards the epicenter (P-waves), (c) fault displacement, (d) orientation of the maximum compressional strain (The closer to the line the better the correlation (dotted lines ±15º).

Tables

Table 1 Summary table showing the main seismic parameters of the Earthquakes of Lorca 2011 (Spain), Emilia Romagna 2012(Italy) and Christchurch 2011 (New Zealand). Data from USGS and IGME, 2011; Martinez-Diaz *et al.,* 2012; Saraò and Peruzza, 2012; Beavan *et al.,* 2012; ISPRA, 2012; Pizzi and Scisciani, 2012; Kaiser *et al.,* 2012; Mckey and Quigley, 2014.

Table 2 Summary table showing the earthquake damage orientation (EDO) for every site and the number of earthquake damage measured in each site; the orientation towards the epicenter (P-waves arrivals), the seismogenic fault trend (0-180º normal to the seismogenic fault plane), orientation of the maximum compressional strain and fault displacement (USGS-focal mechanism).

Table 1

Earthquake sequence	**Events** (Day, Time-UTC)	**Magnitude**	**Location**	**Intensity**	**Moment Tensor**		**Seismogenic fault** (trend, dip, type)	**Surface Rupture**
					Nodal Planes (Strike/Dip/Rake)	**Principal axes** (Azimut)		
Lorca (Spain)	2011-05-11 16:47:25 (UTC)	5.1	37.699°N 1.672°W	VIII	234°/45º/43 111°/61º/126	T=71º; N=271; P 175º	ENE-WSW, 55º - 65° NW, strike-slip with reverse component	No
Emilia Romagna (Italy)	2012-05-20 02:03:52 (UTC)	6.0	44.890°N 11.230°E	VIII	305º/70º/100º 98º/22º/64º	T=249º; N=114º ;P=21º	WNW-ESE, low-dipping S, reverse (Blind trust)	No
	2012-05-29 07:00:03 (UTC)	5.8	44.851°N 11.086°E	VIII	280º/70º/90º 100º/20º/90º	T=222º; N=107º; P=14º	WNW-ESE, low-dipping S, reverse (Blind trust)	No
Christchurch (South Island of New Zealand)	2011-02-21 23:51:42 (UTC)	6.1	43.583°S 172.680°E	IX	165°/ 71°/ 32° 63°/ 60°/ 157°	T=27º; N=193º; P=292º	ENE-WSW, S, reverse with strike slip component	No
	2011-06-13 02:20:49(UTC)	5.9	43.564°S 172.743°E	VIII	161°/ 76°/ 19°; 66°/72°/165°	T=24; N=197º; P=293º	NNW-SSE, left lateral strike slip	No
	2011-12-23 02:18:03 (UTC)	5.9	43.530°S 172.743°	VII	181°/ 62°/47 65°/50°/142°	T=39º; N=205º;P=301	ENE-WSW, S, revers	No

Table 2

Sites	Nº ED	Earthquake orientation damage EDO	EDO (general trend)	Direction to the Epicenter location-(P-waves)	P maximum compressional strain	Fault displacement	Fault trend (normal to)
LORCA 2011 (SPAIN)							
Paso Blanco (Site 1)	61	N335º	NNW-SSE	N45º	N175º	N20º	N144º
Paso Azul (Site 2)	8	N165º	SSE	N40º	N175º	N20º	N144º
Castillo (Site 3)	19	N330º	NNW-SSE	N50º	N175º	N20º	N144º
Cortijo (Site4)	2	N135º	SE	N85º	N175º	N20º	N144º
Uni (Site 5)	5	N150º	NNW-SSE	N35º	N175º	N20º	N144º
San Clemente (Site 6)	65	N155º	NNW-SSE	N40º	N175º	N20º	N144º
EMILIA ROMAGNA 2012(ITALY)							
Mirandola	16	N225º	NNE-SSW	N90º	N21º	N35º	N30º
Massa Finalese	4	N185º	S	N15º	N21º	N0º	N10º
Finale Emilia	18	N210º	NNE-SSW	N145º	N21º	N35	N30º
San Felice sul Panaro	10	N155º	SSE	N130º	N21º	N0º	N10º
Crevalcore	15	N125º	SE and SW	N20º	N21º	N0º	N10º
Cavezzo	27	N175º	S	N65º	N21º	N0º	N10º
San Carlo	6	N45º	NNE-SSW	N130º	N21º	N35º	N30º
CHRISCHURCH 2011(NEW ZEALAND)							
Badoes Cementery	30	N165º	SSE and ENE	N155º	N110º	N151º	N155º
Linwood Cementery	32	N75º	ENE and N	N130º	N110º	N156º	N71º
Addinton Cementery	60	N125º	NNW-SSE	N120º	N110º	N151º	N155º
Bromley Cementery	37	N285º	W-E	N120º	N110º	N156º	N71º
Prebbenton Cementery	1	N165º	SSE	N90º	N110º	N151º	N155º
Woolston Cementery	7	(N170º-250º)	N-SSW	N150º	N110º	N151º	N155º

Highlights

-Earthquake damage orientation (EDO) has been measured and quantify

-EDO analysis versus instrumental data, not possible in archaeological or historical EQ

-It is observed a systematic EDO pattern in the fault trace proximity

-In the near field the EDO is normal to the fault trend (±15º)

-EDO can be used to infer seismic parameters of the seismogenic fault

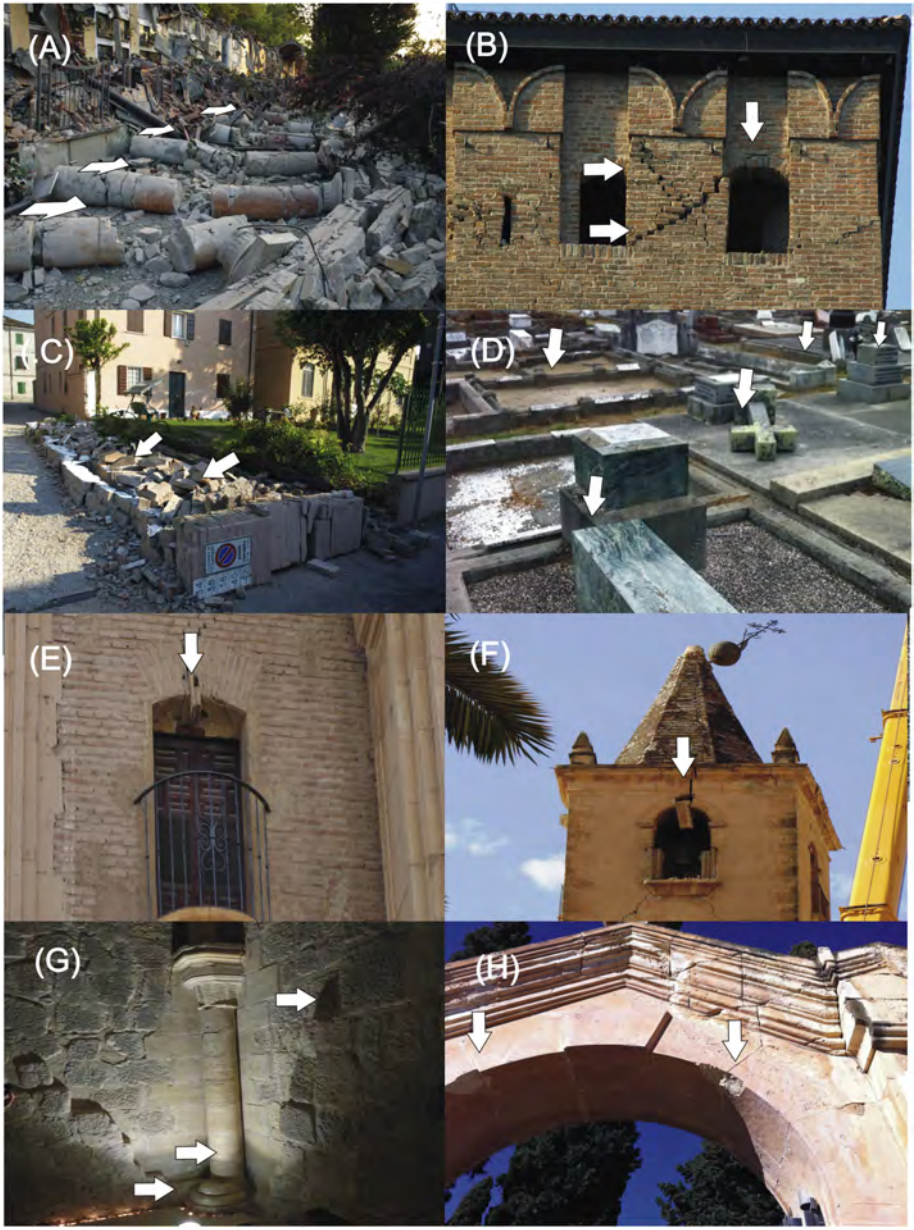

Figure 1

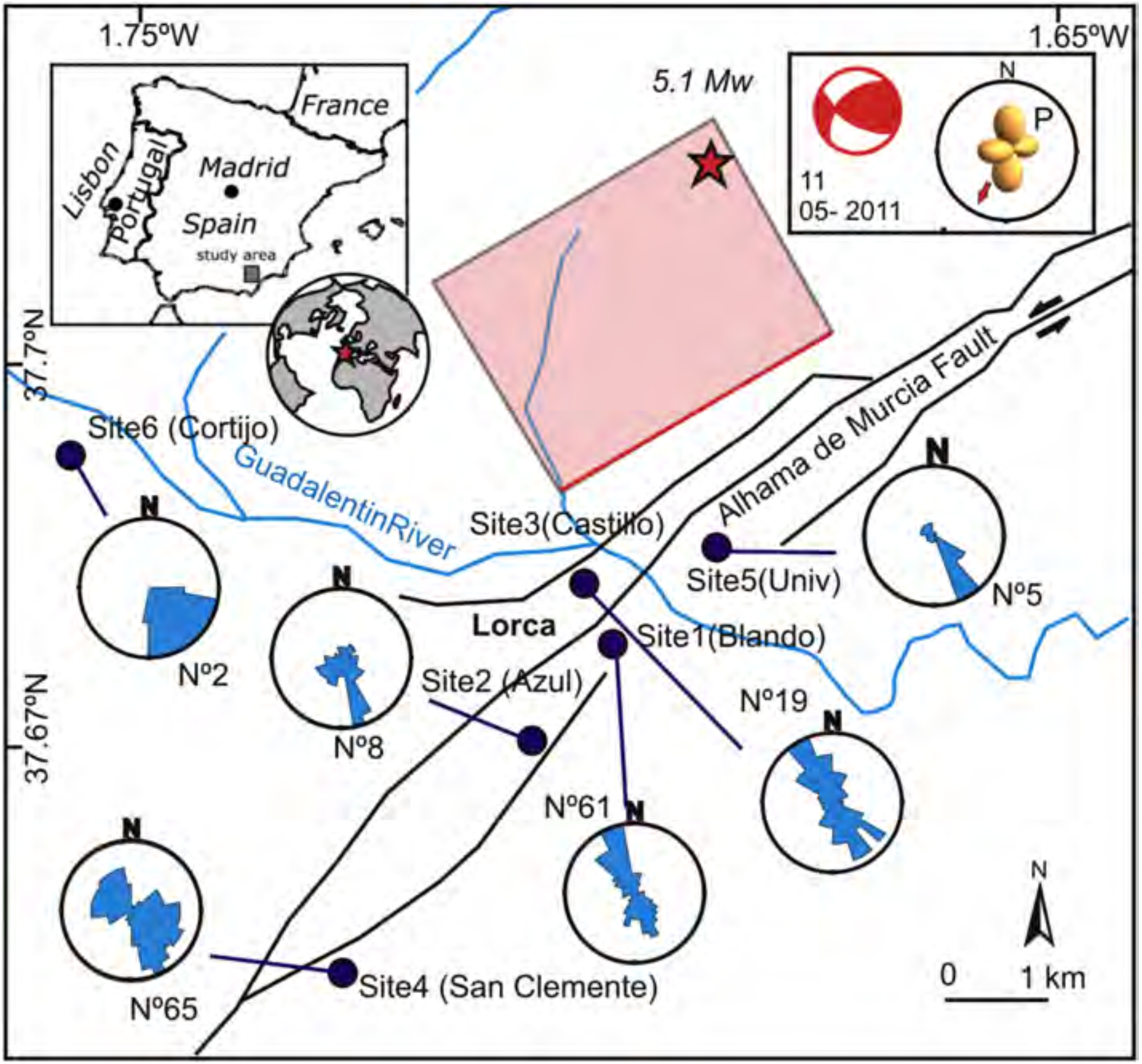
1.75ºW
1.65ºW
5.1 Mw
France
Lisbon
Portugal
Madrid
Spain
study area
11
05- 2011
N
P
37.7ºN
37.67ºN
Site6 (Cortijo)
GuadalentinRiver
Site3(Castillo)
Alhama de Murcia Fault
Site5(Univ)
Nº5
Lorca
Site1(Blando)
Site2 (Azul)
Nº2
Nº8
Nº19
Nº61
Nº65
Site4 (San Clemente)
0
1 km

Figure 2

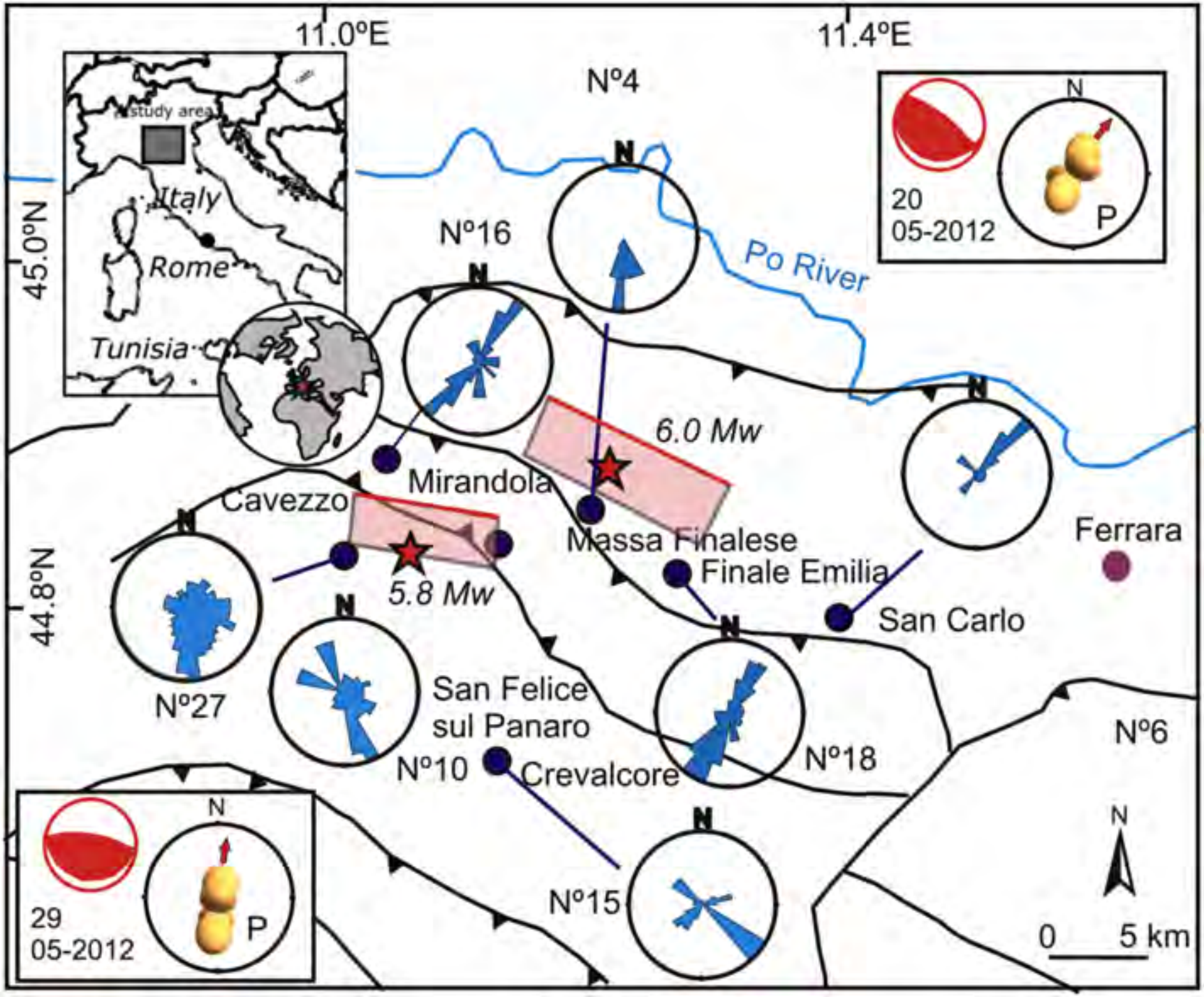
11.0°E
11.4°E
45.0°N
44.8°N
Nº4
Nº16
Nº27
Nº10
Nº15
Nº18
Nº6
study area
Italy
Rome
Tunisia
Po River
6.0 Mw
5.8 Mw
Mirandola
Cavezzo
Massa Finalese
Finale Emilia
San Carlo
Ferrara
San Felice
sul Panaro
Crevalcore
20
05-2012
29
05-2012
P
N
0
5 km

Figure 3

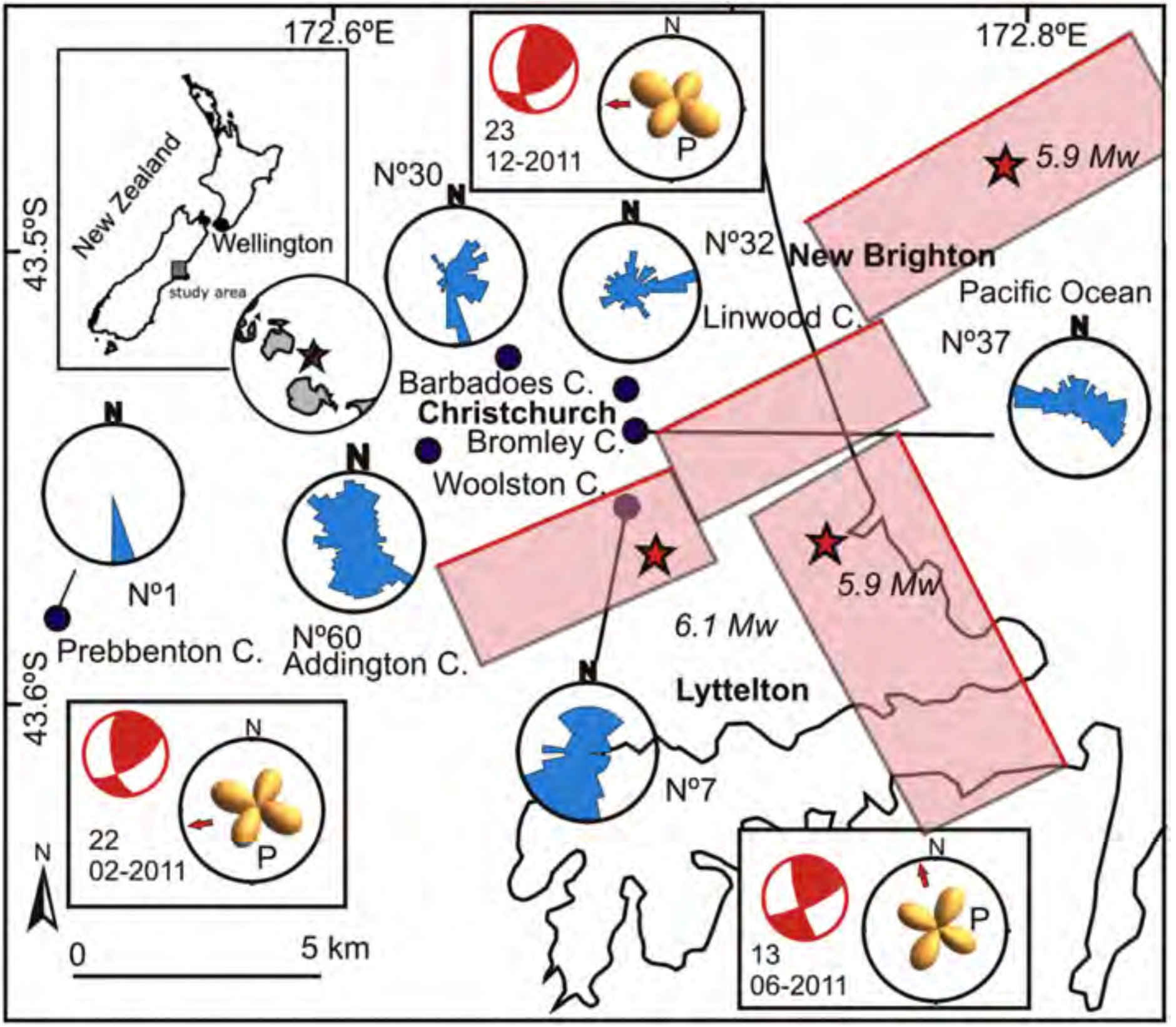
172.6°E
172.8°E
43.5°S
43.6°S
New Zealand
Wellington
study area
23
12-2011
P
N
Nº30
Nº32
Linwood C.
Barbadoes C.
Christchurch
Bromley C.
Woolston C.
New Brighton
5.9 Mw
Pacific Ocean
Nº37
Nº1
Prebbenton C.
Nº60
Addington C.
6.1 Mw
5.9 Mw
Lyttelton
Nº7
22
02-2011
13
06-2011
0
5 km

Figure 4

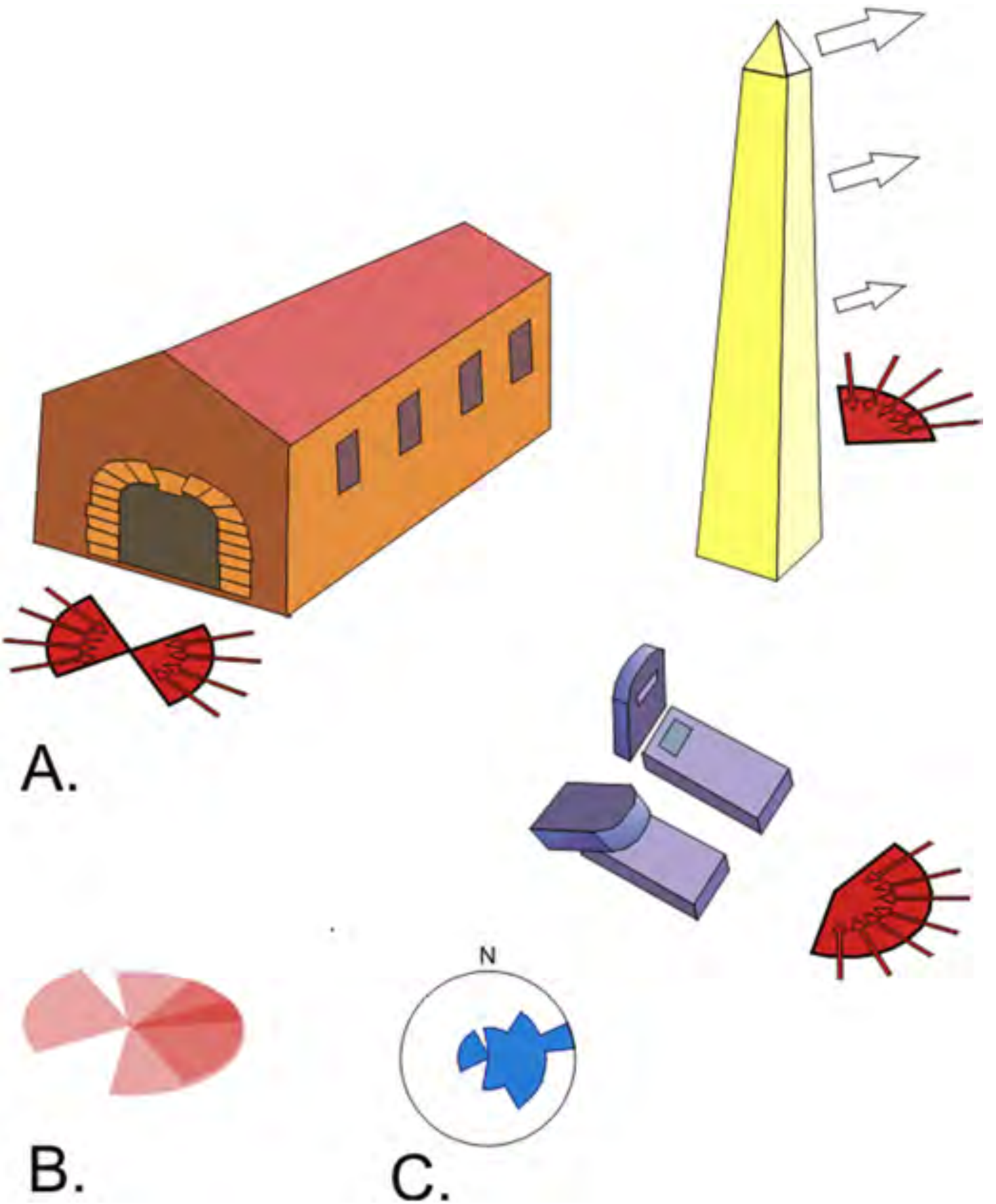

Figure 5

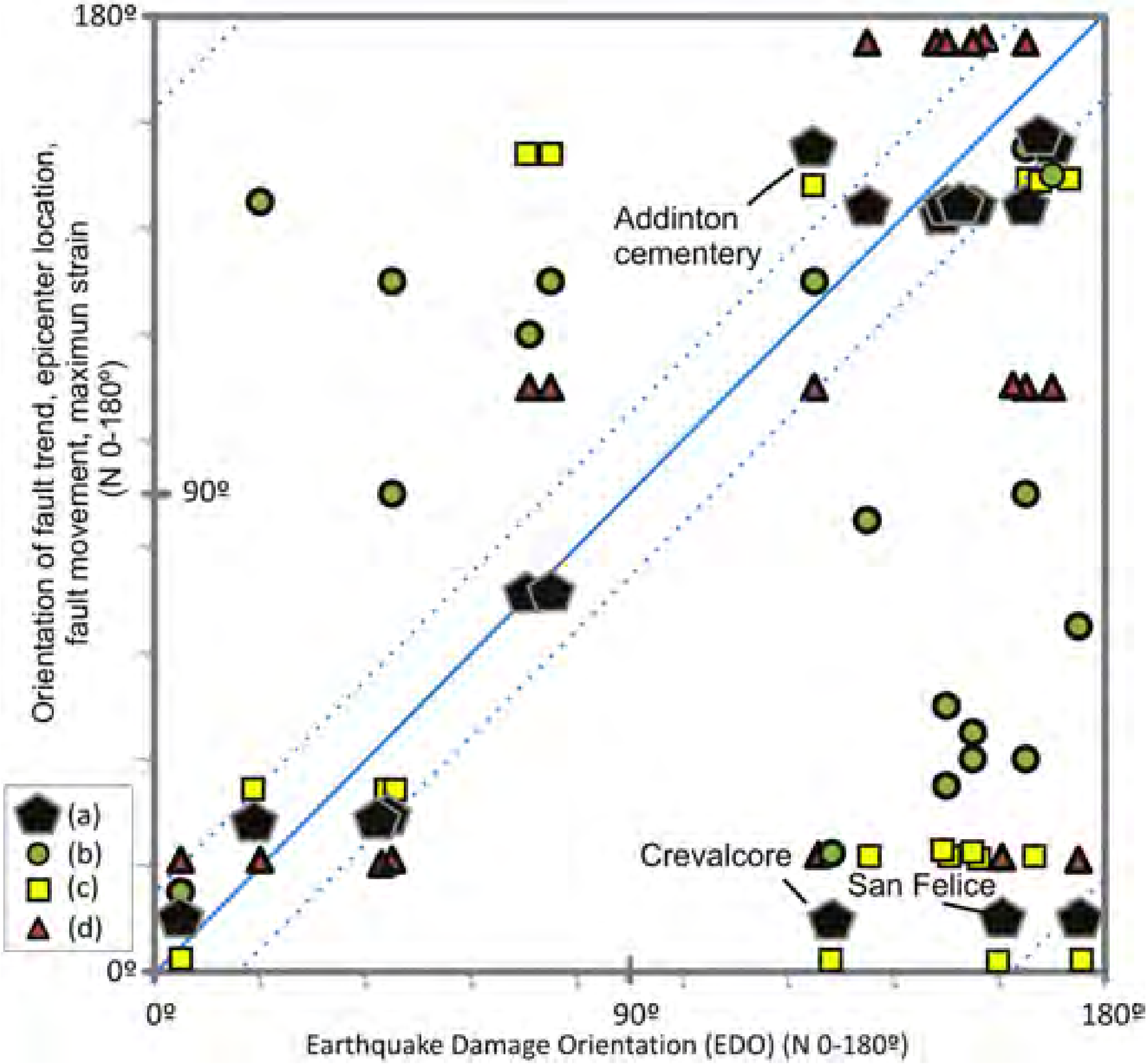
180º
90º
0º
Orientation of fault trend, epicenter location, fault movement, maximun strain (N 0-180º)
Addinton cementery
Crevalcore
San Felice
(a)
(b)
(c)
(d)
0º
90º
180º
Earthquake Damage Orientation (EDO) (N 0-180º)

Figure 6